Non-isothermal crystallization kinetics and stability of leucite and kalsilite from K2O-Al2O3-SiO2 glasses

CHRISTOPOULOU, Georgia, MODARRESIFAR, Farid, ALLSOPP, Benjamin, JONES, Hywel and BINGHAM, Paul <http://orcid.org/0000-0001-6017-0798>

Citation:

Copyright and re-use policy

Non-isothermal crystallization kinetics and stability of leucite and kalsilite from K$_2$O-Al$_2$O$_3$-SiO$_2$ glasses

Georgia Christopoulou[1], Farid Modarresifar[2], Benjamin L. Allsopp[1], Alan H. Jones[1] and

Paul A. Bingham[1]*

[1]*Materials and Engineering Research Institute, Sheffield Hallam University, Howard Street, Sheffield, S1 1WB, UK.*

[2]*Morgan Advanced Materials, Thermal Ceramics UK, Tebay Road, Bromborough, CH62 3PH, UK.*

Abstract

The crystallization mechanisms and elemental stability of leucite and kalsilite formed from K$_2$O-Al$_2$O$_3$-SiO$_2$ glasses were investigated by X-ray powder diffraction (XRD), X-ray fluorescence (XRF), Raman spectroscopy and differential scanning calorimetry (DSC). Glass samples with compositions along the leucite-kalsilite tie-line were produced by melt processing; and were then heat treated at 850ºC, 950ºC and 1250ºC for times ranging from 5 minutes to 1000 hours. Kalsilite is an unstable phase that behaves as an intermediate precursor to leucite. Crystalline materials in which kalsilite is the major phase lose potassium upon prolonged heat treatment (1000 hours at 1250ºC), in contrast to those with leucite, in which little or no compositional alteration is detected. The formation of leucite from stoichiometric kalsilite is accompanied by the formation of potassium doped alumina. The activation energies for leucite and kalsilite crystallization, determined via application of the Kissinger equation to thermal analysis data, were 579 kJ/mol and 548 kJ/mol respectively. Finally, production of pure leucite can be achieved with more favourable crystallization kinetics when starting with off-stoichiometric compositions.

Keywords: kalsilite; leucite; activation energy; reaction mechanism

*Corresponding author.

E-mail: p.a.bingham@shu.ac.uk

1.   Introduction

The ternary system K_2O-Al_2O_3-SiO_2 has received attention because of its fundamental importance to a broad range of disciplines and technologies including mineralogy, silicate ceramics and refractory applications.[1] This ternary system demonstrates high refractoriness, which is attributed to the existence of three potassium aluminosilicate compounds ($K_2O.Al_2O_3.2SiO_2$, $K_2O.Al_2O_3.4SiO_2$ and $K_2O.Al_2O_3.6SiO_2$) with congruent melting points greater than 1600°C.[2-4]

The most commonly used compound within this ternary system is leucite ($K_2O.Al_2O_3.4SiO_2$) due to its optical properties[5-7] - the development of leucite inside glasses in this phase field does not hinder translucency, and the ability to remain entirely crystalline up to its melting temperature[8,9] render it an excellent material for dental applications such as coating different metals and for resin bonded crowns and veneers.[10-15] Kalsilite ($K_2O.Al_2O_3.2SiO_2$) and leucite, due to their high refractoriness, are also used in geopolymers to enable their production as refractory castables.[16] Their physical behaviour is advantageous in respect to acidity, resistance to fire, compressive strength and they are considered as a possible improvement on cement and as a candidate material for the immobilization of hazardous wastes and low / intermediate level radioactive wastes.[17]

1.1 Leucite

Leucite ($KAlSi_2O_6$) is a potassium aluminosilicate mineral that is found in volcanic rocks, has a congruent melting temperature of 1686°C and occurs in two different polymorphs. Peacor[18] showed that when natural leucite is heat treated at 635°C it crystallizes in cubic form (Figure 1b) which has an *Ia3d* space group. Palmer *et al.*[19] found that leucite forms a tetragonal phase at temperatures under 665°C and according to Mazzi *et al.*[20] at room temperature leucite has

an $I4_1/a$ space group (Figure 1a). The above space groups for both polymorphs are confirmed by Walsh, Harrison and Redfern[21].

Studies have reached somewhat different conclusions regarding the phase transition temperature and the exact phase change sequence for leucite. Peacor[18] showed that leucite transforms with a single transition from tetragonal, which is the low temperature form ($I4_1/a$), to cubic which is the elevated temperature form ($Ia3d$). Later, X-ray diffraction experiments revealed the existence of two transitions, at 655°C and 675°C,[22] whereby tetragonal leucite ($I4_1/a$) will transform to an intermediate phase ($I4_1/acd$) before the final transformation to cubic leucite ($Ia3d$).

1.2 Potassium aluminium silicate

Potassium aluminium silicate ($KAlSiO_4$) occurs in different crystalline forms; according to Smith and Tuttle[2] the $K_2O \cdot Al_2O_3 \cdot 2SiO_2$ compound exists in three different crystal structure families: one orthorhombic and two hexagonal. Kalsilite and kaliophilite minerals correspond to the hexagonal form.[23] More recently, six different crystal structures have been confirmed, including synthetic and natural forms of kalsilite and kaliophilite.[24]

Hexagonal kalsilite has a tetrahedral, open framework which appears to be isostructural with that of nepheline and tridymite, with a topological symmetry $P6_3/mmc$.[25] Kalsilite's framework consists of sheets (001) of ordered SiO_4 and AlO_4 tetrahedra which form 6-membered rings (6mR) pointing alternatively up (U) and down (D). Figure 2a shows the structure of a single tetrahedral sheet of kalsilite. The stacking of the sheets along the c-axis is accomplished by connection by the apical oxygen atoms, which nominally lie on special positions on the threefold rotation axis. The tetrahedral 6mR are additionally di-trigonally distorted as the tetrahedra rotate around (001). The form of this rotation will be the same for

all the sheets of the *P31c* polymorph but with reversed form of rotation in the *P6₃* polymorph among adjacent (001) sheets.[26]

On the other hand, orthorhombic kalsilite (KAlSiO₄-O1) typically exhibits twinning and pseudosymmetry, and its crystal symmetry has been reported to be an average orthorhombic structure with *Pnam* and *Pn2₁m* space groups.[26] Gregorkiewitz et al.[27] successfully produced KAlSiO₄-O1 via solid state synthesis and concluded that its framework topology is different from tridymite and its stuffed derivatives. It is built from sheets which consist of 6-membered rings of ordered SiO₄ and AlO₄ tetrahedra in the ab plane, but these ring topologies are not the UDUDUD sequence of tridymite. In the (001) plane there are two types of six-membered rings, UUDUDD and UUUDDD, in a 2:1 ratio (Figure 3). These authors reported that KAlSiO₄-O1 is actually monoclinic with space group *P12₁1* and has two orthorhombic supergroups, *Pn2₁m* and *P2₁2₁2₁*.

KAlSiO₄ melts at temperatures greater than 1700°C and there are no significant difficulties during the chemical reactions needed to produce kalsilite apart from the hygroscopicity of some mixtures and the volatile character of potassium.[28]

1.3 Transformation of kalsilite to leucite

The transformation of kalsilite to leucite has attracted the attention of a number of researchers [29-31] but the exact mechanism remains unclear. As noted previously, leucite is an important mineral used in a wide range of applications, and particularly in the dental field. Elucidating the transformation mechanism of kalsilite to leucite could improve the existing synthesis methods, such as sol–gel[29], salt bath[32], solid state methods[33], hydrothermal[34] and co-precipitation[35] by producing pure leucite via a more convenient and / or economical way. In some studies, in which leucite was synthesized, kalsilite was detected as a non-stable reaction

product that vanishes with prolonged heat treatment. Zhang *et al.*[36] reported that the formation of kalsilite is a transitional stage that leads to crystallization of leucite. In addition, other recent studies are consistent with the view that kalsilite is the precursor of leucite.[37-42] Moreover, in some studies it is indicated that the prolonged heat treatment of natural or synthesized kalsilite at elevated temperatures will gradually lead to a complete conversion to leucite and this phenomenon is believed to relate to the high volatility of potassium.[27,43]

2. Experimental procedures

2.1 Preparation of leucite and kalsilite samples

To explore the crystallization behaviour of kalsilite and leucite, five potassium aluminosilicate glasses with increasing contents of K_2O were prepared through melt processing, with their compositions based on points along the tie-line from the two corresponding compounds in the $K_2O – Al_2O_3 – SiO_2$ phase diagram. As depicted in Figure 4, these glasses were designed at points along the leucite-kalsilite tie-line and their chemical compositions are presented in Figure 4. All inorganic raw materials (Table 1) were weighed according to stoichiometry. The mixtures were melted in a submerged arc furnace for 1 hour at 2000°C. Samples were then poured onto a large steel plate and then annealed at 550°C to relieve internal stresses. Heat treatments of the glass samples were conducted in air using an electric furnace with schedules summarised in Table 3. During the long-term heat treatment experiments (1-1000 hours) the samples were placed into the furnace at room temperature and the furnace was heated to the selected temperature (1250 °C) at a rate of 5°C per minute in air. Samples were then held at the maximum temperature for the relevant time period, then removed from the furnace at this temperature, at set time intervals with an accuracy of ± 2s for 1min and 5min samples; ± 5s for 15min, 30min and 1h samples; ± 5min for the 24h sample; and ± 1h for the 500h and 1000h samples. Additionally, during short-term (1-30

5

minutes) experiments (Table 3) the samples were placed into the furnace at 1250 °C and then also removed at this maximum temperature. A wide range of heat treatment time (1 minute to 1000 hours) was selected in order to examine the formation and evolution of each crystalline phase. The rationale for the short-term experiments was to study the time needed for each composition to transform from amorphous to crystalline. Additionally, the long-term experiments were selected to explore the stability of each crystalline phase and the kalsilite-leucite transformation; and also to explore the possibility that kalsilite would completely transform to leucite upon prolonged heat treatment.

2.2 Activation energy determination by the Kissinger method

The activation energy for crystallization was determined from the exothermic peak temperatures on the DSC curves using the Kissinger method (Eq. 1)[44].

$$ln \frac{a}{T_0^2} = -\frac{E_a}{RT_0} + C \quad (1)$$

where a is the heating rate, E_a is the activation energy, R is the gas constant, T_0 is the exothermic peak temperature in Kelvin and C is a constant. The activation energy is calculated from the slope of the line of $\ln(a/T_0^2)$ vs $1/T_0$ using Fit Multi-Peaks function in the software package Origin.

The shape factor (n) of the exothermic peak is calculated by Eq. 2[45]:

$$n = \frac{2.5}{\Delta T} \cdot \frac{T_0^2}{\left(\frac{E_a}{R}\right)} \quad (2)$$

where n is the Avrami constant and ΔT is the full width at half maximum of the exothermic peak. The value of the Avrami exponent provides information regarding the morphology of the growing crystals[46]. The value of n reveals the dominant mechanism of crystallization.

Smaller values of n indicate that crystallization is controlled by a surface crystallization mechanism instead of volume crystallization, and that the dimension of crystallization is low. The Avrami parameter can be considered to comprise two terms: one that represents the dimension of crystal growth, having integer values of 1, 2 or 3 corresponding to one-, two- or three-dimensional entities that are formed. The second term relates to the time dependence of nucleation with values of either 0 or 1, where 0 corresponds to instantaneous nucleation and 1 to sporadic nucleation[47]. Additionally, larger values of n are expected when increased nucleation rates occur, such as in the diffusion-controlled reaction (>2.5) or the case of polymorphic transformation (>4).[48]

2.3 Sample characterization

Quantitative elemental analysis was carried out with a PANalytical - Axios Advanced for XRF analysis of samples in the form of fused beads: 1.000 ± 0.002g of sample was carefully weighed and mixed with 10.000 ± 0.002g di-lithium tetraborate and formed into a transparent glass disc using an automatic bead making instrument.

Crystallographic evolution after variable heat treatment experiments was investigated by XRD at room temperature, with a diffractometer (model: Empyrean XRD, PANalytical™, Almelo, The Netherlands) equipped with a Cu tube operated at 40 kV and 40 mA, normally in the 2θ range between 5 and 100°, with 2θ increments of 0.013° and counting time of ~70 s per step. All samples were analysed using the reflection spinner sample holder, which spins at 0.25 Hz. All samples were crushed to fine powders using a mortar and pestle prior to measurement.

The thermal behaviour of the samples was investigated by non-isothermal differential scanning calorimetry (DSC). The measurements were performed with a NETZSCH STA 449

F5 Jupiter instrument between room temperature and 1400ºC, with heating rates between $5ºC.min^{-1}$ and $40ºC.min^{-1}$. All DSC measurements were carried out on 50.0 mg samples against the same mass of a 99.9% purity α-Al_2O_3, as the inert reference material, which was calcined at 1450°C for 15 hours.

Raman spectroscopy of glass materials was carried out to elucidate structure and to assist with determining the existence of residual crystalline SiO_2 in crystalline samples. Raman spectra were recorded with a Thermo Scientific™ DXR™2 microscope spectrometer equipped with a laser beam emitting at 532 nm, at 300 mW output power. The photons scattered by the sample were dispersed by a 1200 lines/mm grating monochromator and simultaneously collected on a CCD camera; the collection optic was set at 50× objective.

3   Results

3.1 Structural characterization

Heat treatment experiments of the glasses at 1250°C resulted in multiphase and single-phase crystalline reaction products occurring in the kalsilite-leucite phase fields. The heat treatment temperature was selected on the basis of the DSC results, which showed that the first crystallization event occurred for all the samples at approximately 1250°C. Additionally, the selected heat treatment temperature of 1250°C is below the liquidus temperature for all compositions studied, hence all compositions were expected to crystallise. For short heat treatment times (up to 24 hours), all compositions formed the primary phases expected from the K_2O-Al_2O_3-SiO_2 phase diagram,[49] i.e. samples KAS-1 and KAS-2 formed leucite, KAS-3 and KAS-4 a mixture of leucite and kalsilite, and KAS-5 formed kalsilite. Prolonged heat treatment altered the phases present in some of the samples as discussed below. Heat treatment experiments were conducted to test the stability of leucite (KAS-1) and kalsilite (KAS-5) at 1250°C for up to 1000 hours and to further examine whether the development of

leucite could be achieved from the other samples. Sample KAS-2 formed only leucite so long-term (after 24 hours) experiments were not performed.

X-ray powder diffraction

According to XRD analysis (Figure 5 and Figure 6), samples KAS-1 and KAS-2 are X-ray amorphous prior to heat treatment. After heat treatment at 1250°C for up to 1000 hours and 24 hours, respectively, they both formed only tetragonal leucite (ICDD 01-076-8737) without any phase transformation or development of second phases.[50] This suggests that leucite is a stable crystalline phase in terms of time at 1250°C. Crystallization of leucite occurs very rapidly, in less than 5 minutes for sample KAS-1 and less than 15 minutes for sample KAS-2.

Figure 7 shows the crystallization behaviour of sample KAS-1 as a function of temperature for 1 hour of heat treatment. At 850°C kalsilite peaks are stronger compared to those of leucite, with high levels of amorphous phase remaining. At higher temperature (950°C) the proportion of leucite increases and kalsilite is still present, and there is little, if any, amorphous phase. At even more elevated temperatures (1250°C), kalsilite is not detectable and leucite is the sole crystalline phase, with no evidence of amorphous phase.

As shown in Figure 8 for sample KAS-3, orthorhombic potassium aluminium silicate, kalsilite[51], (ICDD 00-033-0988) and tetragonal leucite peaks form simultaneously, as suggested by the phase diagram wherein the composition of KAS-3 lies on a phase field boundary. The quantity of kalsilite decreases with increasing heat treatment times and as tetragonal leucite forms but at 1000 hours it does not appear to have reduced any further suggesting that an equilibrium has been achieved. The crystallization process for sample KAS-3 takes longer (< 30 minutes) than for samples KAS-1 and KAS-2.

In the initial stage of crystallization of samples KAS-4 and KAS-5 at 1250°C, hexagonal kalsilite (ICDD 00-012-0134)[2] is formed, which then inverts to orthorhombic kalsilite, with this transition being detected by XRD after about 24 hours (KAS-4) and 500 hours (KAS-5) of heat treatment (Figure 9 and Figure 10). Capobianco et al.[43] obtained orthorhombic kalsilite by annealing natural hexagonal kalsilite at 1200°C in open Pt crucibles for 48 hours, which is not inconsistent with our results. The complete transition from hexagonal to orthorhombic kalsilite is accompanied by the formation of leucite after between 1 hour and 24 hours of heat treatment at 1250°C, as observed in the XRD patterns shown in Figure 9 and Figure 10. It is unclear whether hexagonal kalsilite first transforms to orthorhombic kalsilite which then gradually transforms to leucite, or whether orthorhombic kalsilite and leucite form simultaneously.

For sample KAS-4, Figure 9 illustrates that at the beginning of crystallization most of the diffraction peaks are matched by hexagonal kalsilite. After 24 hours of heat treatment at 1250°C only tetragonal leucite and orthorhombic kalsilite are present. Moreover, crystallization occurs rapidly, in less than 15 minutes. Once again, kalsilite gradually transforms to leucite with increasing heat treatment time at 1250°C.

In the early stages of crystallization (< 24 hours) for sample KAS-5 (Figure 10) hexagonal kalsilite forms, which then transforms into orthorhombic kalsilite with simultaneous formation of tetragonal leucite and hexagonal potassium aluminium oxide (ICDD 04-010-8954) which is also known as potassium doped alumina ($KAl_{11}O_{17}$) or K-β-alumina[52]. The unstable nature of kalsilite is also described in other studies[29,30,36] which show that it probably acts as a precursor of leucite. Even for sample KAS-5, which has the kalsilite stoichiometry, a small amount of leucite forms after prolonged heat treatment. In the aforementioned studies which aimed to produce pure leucite (with silica-rich starting compositions), kalsilite crystallised first at lower temperatures (800°C) and transformed to leucite as the temperature

increased (900°C). It is important to stress that our study confirms that during the transformation of kalsilite to leucite, K-β-alumina is also formed. To our knowledge this has not been previously reported, and its formation may modify the properties of the products produced via the kalsite-to-leucite conversion. The main diffraction peak from K-β-alumina is at ca. 7° 2θ: in the aforementioned studies where this phase transformation was examined, reported XRD data started from 10° 2θ, which may explain why K-β-alumina has not previously been associated with the kalsilite-leucite phase transition.

Raman spectroscopy

Raman spectroscopy was used to characterize the structure of glass and crystalline materials. Raman spectra (Figure 11a) of as-annealed glass samples show the presence of Raman bands which occur in the ranges of ca. 300-650 cm^{-1}, and 700-1200 cm^{-1}. The Raman band at 525-625 cm^{-1} is attributed to bending symmetric vibrations of (Si, Al)-O tetrahedra and the peak at 400-525 cm^{-1} is related to bending vibrations of Al−O− and Si−O−[53]. It is well established[53-55] that the broad Raman band at 900-1200 cm^{-1} is typical for silicate and aluminosilicate glasses and is attributed to to Si-O and Al-O Q^n units of the tetrahedral network. The large width of these bands confirms the high presence of amorphous phase in the examined materials, and also a distribution of Q-species consistent with a depolymerised tetrahedral amorphous network. The gradual shift to lower Raman shifts of the overall peak position and profile, on moving from sample KAS-1 to KAS-5, is fully consistent with the increasing network modifier oxide (K_2O) through this series, confirming increasing depolymerisation of the aluminosilicate network from sample KAS-1 to KAS-5. A peak around 1020 cm^{-1} which is present in the spectra for samples KAS-4 and KAS-5, and which is more prominent in the spectrum for sample KAS-3 is attributed to impurities in the

materials and, more specifically, residual or reaction product carbonate[56]. Oxide glasses with high K_2O contents have the tendency to react with the atmosphere and form K_2CO_3.

Figure 11b shows Raman spectra demonstrating the effects of heat treatment on glass samples which exhibit stronger, sharper Raman bands consistent with the existence of crystalline phases. All samples were fired at 1250°C for 24 hours before being analysed. Samples KAS-1 and KAS-2 produce Raman spectra corresponding to tetragonal leucite[57]. As confirmed by XRD, samples KAS-3 and KAS-4 form orthorhombic kalsilite whilst sample KAS-5 forms hexagonal kalsilite. The authors were unable to find any existing literature data regarding the Raman spectrum of orthorhombic kalsilite. Hexagonal kalsilite[28] is expected to show a sharp band at around 300-400 cm^{-1} and a group of low intensity bands in the range 900-1050 cm^{-1}. The Raman spectrum of sample KAS-5 is not the same as that of hexagonal kalsilite. The observed modes in the ranges of ca. 240-260 cm^{-1}, 275-325 cm^{-1}, 350-370 cm^{-1}, 380-400 cm^{-1}, 450-470 cm^{-1} and 900-950 cm^{-1} for samples KAS-3, KAS-4 and KAS-5 cannot be fully identified, however, some or all of them may be attributable to orthorhombic kalsilite. The presence of high frequency modes at 1000-1200 cm^{-1} could be related to residual aluminosilicate glass and could also be evidence of small amounts of residual silica in these samples.

3.2 Chemical characterization

Elemental analysis (XRF) revealed (Table 4) that in samples KAS-1 and KAS-2, which have compositions in the leucite phase field (SiO_2-rich), no potassium loss was observed after heat treatment at 1250°C. Additionally, for sample KAS-3, the next closest material to the composition of leucite, potassium loss was significantly lower (1.5 wt%) compared to the samples (KAS-4 and KAS-5) with compositions closer to the stoichiometry of kalsilite (2.7-3.6 wt%) for the same heat treatment conditions.

These results suggest that chemical stability is strongly connected with the starting composition and hence the amount of kalsilite formed at 1250°C, since apart from the starting chemical composition all of the remaining experimental conditions (electric furnace, temperature and heat treatment duration) and the analysis settings (XRF calibration and fused bead sample making) were identical for all the samples under investigation. It is important to note that even though the XRF results are presented as oxides, in the case of potassium loss it is unclear in which chemical form the potassium is volatilised or evolved.

3.3 Thermal analysis

Non-isothermal differential thermal analysis was employed to explore the crystallization behaviour of glass samples and determine the activation energy of crystallization. As depicted in Figure 12, DSC curves show one strong exothermic peak related to the main crystallization event. The main exothermic peak for samples KAS-1, KAS-2 and KAS-3 relates to the development of leucite. For these three samples, a strong anomaly is observed just before the first crystallization event, which may relate to an endothermic event, probably a rearrangement of the structure of the amorphous phase. Also, moving from the leucite phase field glass samples KAS-1 to KAS-3, the first crystallization exotherm moves to higher temperatures. This is contrary to the kalsilite phase field glasses, KAS-4 and KAS-5, for which it moves to lower temperatures. The exotherm of sample KAS-1 at a heating rate 5°C/min was extremely weak so it was not included in the results presented here.

As depicted in all DSC curves, all of the exothermic peaks increase in intensity, become broader and shift to higher temperatures with increasing heating rate. According to Kissinger [44] and Speil et al.[58] the heating rate ($\Phi = \frac{dT}{dt}$), affects the temperature and shape of DSC peaks. The peaks become wider because at higher heating rates the spatial gradient of

temperature in the sample will increase. At a higher Φ, the reaction in the sample requires less time.

According to XRD data, when samples KAS-3, KAS-4 and KAS-5 were heat treated at 1250°C the formation of the primary crystallization phase occurs rapidly and then a second phase appears at longer heat treatment times. DSC results (Figure 12f) show only one crystallization event for these materials as the formation of a second phase is both temperature- and time-dependent. For instance, in the case of leucite (KAS-1) XRD shows that kalsilite will develop first, at around 850°C, and then leucite will develop at higher temperature. However, for this to be accomplished the sample must be heat treated at this temperature for 1 hour, which explains the differences between the two measurements.

The calculated activation energy of crystallization varies considerably for the different samples. It is 579±8 kJ/mol for KAS-1 (stoichiometric leucite), decreasing to 473±1 kJ/mol, 364±1 kJ/mol and 360±1 kJ/mol for samples KAS-2, KAS-3 and KAS-4 respectively, then increasing again to 548±1 kJ/mol for sample KAS-5 (stoichiometric kalsilite), indicating that the formation of kalsilite is kinetically favoured. For the glass samples with intermediate compositions, the activation energies are much lower, as shown in Figure 13, with the lowest activation energies (samples KAS-3 and KAS-4, 364 and 360 kJ/mol) determined for the samples which are compositionally furthest away from the stoichiometric compounds. It is believed[59,60] that if the melt and the crystal are identical in composition, the crystal growth rate is controlled by interface reactions, but if the composition of the melt differs to that of the crystal, both interdiffusion and the interface reactions can control crystal growth which may explain the lower activation energies for the KAS-2 sample and particularly for the KAS-3 and KAS-4 samples.

The combined average shape factor (Avrami constant) was similar, as depicted in Table 5, for all sample data, which indicates that the crystal formation process for all samples is three-dimensional growth and nucleation which follows the diffusion-controlled mechanism with increasing nucleation rate.[48] The three-dimensional nucleation and crystal growth mechanism for kalsilite and leucite samples has also been reported in other studies.[36,37,61]

4 Discussion

This study aimed to develop an understanding of the transformation mechanism of kalsilite to leucite, the thermal stability of both phases and the feasibility of producing leucite from different starting compositions. XRD analysis has demonstrated that kalsilite is unstable at elevated temperatures (1250°C) and will transform into leucite as a function of time, as also reported in the literature.[27,43]

The glasses with chemical compositions falling within the kalsilite phase field (samples KAS-4 and KAS-5) primarily form kalsilite as expected. Then, after prolonged heat treatment – with the exact time varying depending on composition – kalsilite transforms to leucite with an accompanying loss of potassium as measured by XRF. There are two proposed potential routes for the transformation of kalsilite to leucite in a compositional system inside the leucite-kalsilite phase fields, as follows:

(i) The first hypothesis is that K_2O and Al_2O_3 are ejected from kalsilite according to Eq. 3:

$$KAlSiO_4 \rightarrow \frac{1}{4}K_2O + \frac{1}{4}Al_2O_3 + \frac{1}{2}(KAlSi_2O_6) \quad (3)$$
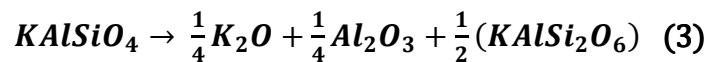
This mechanism shows that after prolonged heat treatment, kalsilite will completely transform to leucite, particularly in the case of stoichiometric kalsilite. In this case some of the ejected potassium will react with alumina to form K-β-alumina, and the remainder will

15

evaporate, according to Eq. 4. Again, it is not confirmed in which chemical form the potassium volatilises, but we have depicted it here as K_2O.

$$\frac{3}{2}K_2O + \frac{11}{2}Al_2O_3 \rightarrow KAl_{11}O_{17} + K_2O \uparrow \quad (4)$$
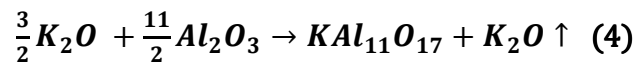
The formation of potassium aluminium oxide, or K-β-alumina, has been confirmed by XRD for KAS-5 samples when heat treated at 1250°C and seems to be more applicable only for the samples that are stoichiometrically close to kalsilite. The formation of this K-β-alumina is related to the starting composition and the excess of alumina in the system and is not observed when leucite is formed from its stoichiometric mixtures. The formation of K-β-alumina, as described in Eq. 4, requires significantly more alumina than potassium oxide; thus if this excess of alumina is not present, the ejected potassium may evaporate without K-β-alumina forming, as occurs in the case of sample KAS-4 sample, where even though the potassium loss is higher than for sample KAS-5, K-β-alumina is not formed.

(ii) The second hypothesis is that the transformation mechanism follows the reaction shown in Eq. 5:

$$KAlSiO_4 + SiO_2 \rightarrow KAlSi_2O_6 \quad (5)$$
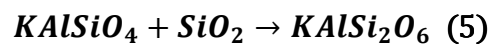
This hypothesis is analogous to the crystallization mechanism of mullite as reported in literature.[62,63] There, the first crystalline phase formed is spinel, which reacts with the SiO_2-rich amorphous phase to form mullite ($Al_6Si_2O_{13}$) at elevated temperatures (1000°C). Correspondingly, $KAlSiO_4$ would react with residual SiO_2 and transform to $KAlSi_2O_6$. This is consistent with the XRD results presented in this study for KAS-5 samples heat treated at 1250°C for 1000 hours. Phase transformation of the first crystallization product with amorphous SiO_2 from the residual glass phase was also reported in other alkali aluminosilicate systems (Li_2O-Al_2O_3-SiO_2) wherein the first nucleation product is Li_2SiO_3 which develops at 650°C, and then at 830°C it reacts with residual SiO_2 to form $Li_2Si_2O_5$.[64,65]

XRD results do not indicate the presence of residual silica in the KAS-3 to KAS-5 samples which is important for the second mechanism, however, Raman spectroscopy has indicated the presence of some retained silicate glass for samples KAS-3, KAS-4 and KAS-5.

XRF and XRD analyses for samples KAS-3 to KAS-5 at 1250°C and sample KAS-1 at 850°C demonstrated that kalsilite will nucleate first; and then between 24 and 500 hours of heat treatment the development of leucite, and in some cases potassium aluminium oxide (K-β-alumina) is accompanied by the evaporation of potassium. Kalsilite will transform to leucite by reacting with SiO_2 from the amorphous phase. This reaction will create in the system an excess amount of potassium and aluminium. In addition, some of the potassium will react with the remaining aluminium forming potassium aluminium oxide (K-β-alumina) and the rest will evaporate as described in Eq.4. Both possible transformation mechanisms (i and ii) indicate that kalsilite is an unstable phase that with time will transform into leucite at 1250°C.

The second transformation mechanism is also possible in the case of sample KAS-1 (leucite composition) where at lower temperatures kalsilite is initially formed (Figure 7). XRF (Table 4) reveals that sample KAS-1 will not have any elemental alteration as a function of heat treatment time. Again, the first crystallization product is kalsilite at low temperatures, which will react with the SiO_2 in the amorphous phase to form leucite (Eq. 5). The starting glass compositions are potassium-deficient compared to kalsilite, which may explain why there is no loss of potassium in this case. XRD results suggest that these reactions will continue until all kalsilite transforms to leucite at elevated temperatures. As other studies in the formation of leucite have indicated,[31,36,66] having adequate crystallization kinetics, a metastable phase – in this case kalsilite – can form first. Indeed, Zhang et al.[36] determined by the Kissinger method[44] that the activation energy for crystallization of kalsilite is lower than that of leucite, which is consistent with the results of this work. According to Abbot[67] orthorhombic kalsilite

is more likely to be a metastable phase. Nucleation and growth kinetics can be altered by the addition of nucleating agents[29,31,68] such as leucite nanocrystals, which lead to the elimination of kalsilite as an intermediate crystallization product, and the formation of leucite at lower temperatures. It is important to note that, as this study has shown, the formation of leucite is possible with any starting composition along the leucite-kalsilite tie-line; especially here for sample KAS-2 with leucite as the sole crystalline phase, the activation energy is significantly lower (by 100 kJ/mol) compared with sample KAS-1. This finding can have important implications for the production of pure leucite materials in future.

5   Conclusions

Heat treatment of glasses in the ternary K_2O-Al_2O_3-SiO_2 system has revealed that kalsilite is an unstable phase at 1250°C and that it behaves as an intermediate precursor of leucite. Leucite begins to develop from kalsilite either with increasing temperature for samples close to leucite stoichiometry or with increasing time at 1250°C for the samples close to kalsilite stoichiometry. Samples in which kalsilite is the main phase lose potassium after prolonged heat treatment (1000 hours) as opposed to samples in which leucite is the major phase formed at 1250°C, in which no compositional alteration was detected with time or temperature.

Two hypotheses have been presented regarding the phase transformation of kalsilite to leucite and the evaporation of potassium. In the first, potassium and aluminium are ejected from unstable kalsilite, resulting in a more stable phase which is leucite. In the second hypothesis, unstable kalsilite reacts with residual SiO_2 to form a more stable phase which is leucite. For both mechanisms, in the case of the stoichiometric kalsilite sample (KAS-5) the excess potassium evaporates, and some reacts with the additional aluminium oxide existing in the system (KAS-5) to form $KAl_{11}O_{17}$ (K-β-alumina). Taking into consideration the results of this study, in combination with literature, it seems more likely that the second mechanism is

taking place during this phase transformation. Finally, production of pure leucite can be achieved with more favourable crystallization kinetics when starting with off-stoichiometric compositions.

Acknowledgements

References

1. Heimann RB. *Classic and advanced ceramics: from fundamentals to applications.* Weinheim: John Wiley & Sons; 2010.

2. Smith JV, Tuttle OF. The nepheline-kalsilite system; Part I, X-ray data for the crystalline phases. Am J Sci. 1957;255(4):282-305.

3. Schairer JF, Bowen NL. The system $K_2O-Al_2O_3-SiO_2$. Am J Sci. 1955;253(12):681-746.

4. Yazhenskikh E, Hack K, Müller M. Critical thermodynamic evaluation of oxide systems relevant to fuel ashes and slags, Part 5: Potassium oxide–alumina–silica. CALPHAD. 2011;35(1):6-19.

5. Bagis B, Turgut S. Optical properties of current ceramics systems for laminate veneers. J Dent. 2013;41:24-30.

6. Weber MJ. *Handbook of optical materials.* London: CRC press; 2003.

7. Raptis NV, Michalakis KX, Hirayama H. Optical behavior of current ceramic systems. Int J Periodont Rest Dent. 2006;26(1):31-41.

8. Isgro G, Kleverlaan CJ, Wang H, Feilzer AJ. The influence of multiple firing on thermal contraction of ceramic materials used for the fabrication of layered all-ceramic dental restorations. Dent Mater. 2005;21(6):557-564.

9. Morena R, Lockwood PE, Fairhurst CW. Fracture toughness of commercial dental porcelains. Dent Mater. 1986;2(2):58-62.

10. El-Meliegy E, van Noort R. *Glasses and glass ceramics for medical applications.* New York: Springer science & business media; 2011.

11. Denry I, Holloway JA. Ceramics for dental applications: a review. Materials. 2010;3(1):351-368.

12. Chatzistavrou X, Esteve D, Hatzistavrou E, Kontonasaki E, Paraskevopoulos K, Boccaccini A. Sol–gel based fabrication of novel glass-ceramics and composites for dental applications. Mat Sci Eng, C. 2010;30(5):730-739.

13. Höland W, Rheinberger V, Apel E, van't Hoen C, Höland M, Dommann A, et al. Clinical applications of glass-ceramics in dentistry. J Mater Sci: Mater Med. 2006;17(11):1037-1042.

14. Cattell MJ, Chadwick TC, Knowles JC, Clarke RL, Samarawickrama DY. The nucleation and crystallization of fine grained leucite glass-ceramics for dental applications. Dent Mater. 2006;22(10):925-933.

15. Fabianelli A, Pollington S, Papacchini F, Goracci C, Cantoro A, Ferrari M, et al. The effect of different surface treatments on bond strength between leucite reinforced feldspathic ceramic and composite resin. J Dent. 2010;38(1):39-43.

16. Bell JL, Driemeyer PE, Kriven WM. Formation of ceramics from metakaolin□based geopolymers. Part II: K□based geopolymer. J Am Ceram Soc. 2009;92(3):607-615.

17. Kamseu E, Rizzuti A, Leonelli C, Perera D. Enhanced thermal stability in K_2O-metakaolin-based geopolymer concretes by Al_2O_3 and SiO_2 fillers addition. J Mater Sci. 2010;45(7):1715-1724.

18. Peacor DR. A high temperature single crystal diffractometer study of leucite, $(K,Na)AlSi_2O_6$. Z Krist-New Cryst St. 1968;127(1-4):213-224.

19. Palmer DC, Dove MT, Ibberson RM, Powell BM. Structural behavior, crystal chemistry, and phase transitions in substituted leucite: High-resolution neutron powder diffraction studies. Am Mineral. 1997;82(1-2):16-29.

20. Mazzi F, Galli E, Gottardi G. The crystal structure of tetragonal leucite. Am Mineral. 1976;61(1-2):108-115.

21. Walsh J, Harrison R, Redfern S. Anelastic behaviour of leucite $KAlSi_2O_6$. Mat Sci Eng, A. 2006;442(1):208-211.

22. Ito Y, Kuehner S, Ghose S. The structure of a high temperature phase in a cationic conductor, $KAlSi_2O_6$. Solid State Ionics. 1995;79:120-123.

23. Buerger MJ. The stuffed derivatives of the silica structures. Am Mineral. 1954;39(7-8):600-614.

24. Okamoto Y. Structural modification of $KAlSiO_4$ minerals. Okayama Univ Earth Sci Reports. 1997;4(1):41-72.

25. Gatta GD, Angel RJ, Zhao J, Alvaro M, Rotiroti N, Carpenter MA. Phase stability, elastic behavior, and pressure-induced structural evolution of kalsilite: A ceramic material and high-T/high-P mineral. Am Mineral. 2011;96(8-9):1363-1372.

26. M. Gregorkiewitz and H. Schäfer. *The structure of $KAlSiO_4$-kaliophilite-O1: Application of the subgroup-supergroup relations to the quantitative space group determination of pseudosymmetric crystals.* Sixth European Crystallographic Meeting; 1980.

27. Gregorkiewitz M, Li Y, White TJ, Withers RL, Sobrados I. The structure of "orthorhombic" $KAlSiO_4$-O1: evidence for Al–Si order from MAS NMR data combined with Rietveld refinement and electron microscopy. Can Mineral. 2008;46(6):1511-1526.

28. Uchida H, Downs RT, Yang H. Crystal-chemical investigation of kalsilite from San Venanzo, Italy, using single-crystal X-ray diffraction and Raman spectroscopy. Geochim Cosmochim Ac. 2006;70(18):677-680.

29. Erbe EM, Sapieszko RS, inventors. 3M Co, assignee. *Chemically derived leucite.* United States patent 5622551. 1997 April 22.

30. Liu C, Komarneni S, Roy R. Seeding effects on crystallization of $KAlSi_3O_8$, $RbAlSi_3O_8$, and $CsAlSi_3O_8$ gels and glasses. J Am Ceram Soc. 1994;77(12):3105-3112.

31. Zhang Y, Wu J, Rao P, Lv M. Low temperature synthesis of high purity leucite. Mater Lett. 2006;60(23):2819-2823.

32. Oishi S, Miyata T, Suzuki T. Growth of leucite crystals from a $K_2Mo_2O_7$ flux. J Mater Sci Lett. 2003;22(13):927-929.

33. Höland W, Frank M, Rheinberger V. Surface crystallization of leucite in glasses. J Non-Cryst Solids. 1995;180(2-3):292-307.

34. Novotna M, Satava V, Kostka P, Lezal D, Maixner J, Klouzkova A. Synthesis of leucite for application in dentistry. Glass Technol. 2004;45(2):105-107.

35. Sheu T, O'Brien W, Rasmussen S, Tien T. Mechanical properties and thermal expansion behaviour in leucite containing materials. J Mater Sci. 1994;29(1):125-128.

36. Zhang Y, Lv M, Chen D, Wu J. Leucite crystallization kinetics with kalsilite as a transition phase. Mater Lett. 2007;61(14-15):2978-2981.

37. Buljan I, Kosanović C, Subotić B, Novak Tušar N, Ristić A, Gabrovšek R, et al. Kinetic analysis of isothermal crystallization of potassium aluminosilicate ceramics (leucite and kalsilite) from amorphous potassium aluminosilicate precursors. Cryst Growth Des. 2010;10(2):838-844.

38. Becerro AI, Escudero A, Mantovani M. The hydrothermal conversion of kaolinite to kalsilite: Influence of time, temperature, and pH. Am Mineral. 2009;94(11-12):1672-1678.

39. Kumar PH, Singh VK, Kumar P. Mechanochemically synthesized kalsilite based bioactive glass-ceramic composite for dental veneering. Appl Nanosci. 2017;7(6):269-274.

40. Kumar P, Srivastava A, Kumar V, Singh H, Sharma S, Kumar P, et al. Role of CaF_2 on mechanochemically synthesized leucite as dental veneering glass ceramics. Adv Appl Ceram. 2015;114(2):107-113.

41. Yin L, Stoll R. *Ceramics in restorative dentistry.* In: Low IM, editor. Advances in Ceramic Matrix Composites United Kingdom: Woodhead Publishing Limited; 2014. p. 624-655.

42. Xie N, Bell J, Kriven WM. Fabrication of Structural Leucite Glass–Ceramics from Potassium⁪Based Geopolymer Precursors. J Am Ceram Soc. 2010;93(9):2644-2649.

43. Capobianco C, Carpenter M. Thermally induced changes in kalsilite ($KAlSiO_4$). Am Mineral. 1989;74(7-8):797-811.

44. Kissinger HE. Reaction kinetics in differential thermal analysis. Anal Chem. 1957;29(11):1702-1706.

45. Avrami M. Kinetics of Phase Change. II Transformation⁪Time Relations for Random Distribution of Nuclei. J Chem Phys. 1940;8(2):212.

46. Johnson BR, Kriven WM, Schneider J. Crystal structure development during devitrification of quenched mullite. J Eur Ceram Soc. 2001;21(14):2541-2562.

47. Augis JA, Bennett JE. Calculation of the Avrami parameters for heterogeneous solid state reactions using a modification of the Kissinger method. J Therm Anal. 1978;13(2):283-292.

48. Takei T, Kameshima Y, Yasumori A, Okada K. Crystallization kinetics of mullite from Al_2O_3–SiO_2 glasses under non-isothermal conditions. J Eur Ceram Soc. 2001;21(14):2487-2493.

49. Osborn EF, Muan A. *Phase equilibrium diagrams of oxide systems.* Columbus, Ohio: American Ceramic Society with the Edward Orton Jr. Ceramic Foundation; 1960.

50. Gatta GD, Rotiroti N, Ballaran TB, Pavese A. Leucite at high pressure: Elastic behavior, phase stability, and petrological implications. Am Mineral. 2008;93(10):1588-1596.

51. Cook LP, Roth RS, Parker HS, Negas T. The system K_2O-Al_2O_3-SiO_2. Part 1. Phases on the $KAlSiO_4$-$KAlO_2$ join. Am Mineral. 1977;62(11-12):1180-1190.

52. Dernier P, Remeika J. Structural determinations of single-crystal K β-alumina and cobalt-doped K β-alumina. J Solid State Chem. 1976;17(3):245-253.

53. McMillan P, Piriou B. Raman spectroscopic studies of silicate and related glass structure—a review. Bulletin de Mineralogie. 1983;106(5):7-75.

54. Devine R. Densification□induced infrared and Raman spectra variations of amorphous SiO^2. J Vac Sci Technol A. 1988;6(6):3154-3156.

55. Yadav AK, Singh P. A review of the structures of oxide glasses by Raman spectroscopy. RSC Advances. 2015;5(83):67583-67609.

56. Ferrari AC, Robertson J. Interpretation of Raman spectra of disordered and amorphous carbon. Phys Rev B. 2000;61(20):14095.

57. Palmer DC, Bismayer U, Salje EKH. Phase transitions in leucite: Order parameter behaviour and the Landau potential deduced from Raman spectroscopy and birefringence studies. Phys Chem Miner. 1990;17(3):259-265.

58. Speil S, Berkelhamer LH, Pask JA, Davies B. Differential thermal analysis of clays and aluminous minerals. *U.S. Bureau of Mines Technical Paper #664.* 1945;664:81.

59. MacFarlane DR, Matecki M, Poulain M. Crystallization in fluoride glasses: I. Devitrification on reheating. J Non-Cryst Solids. 1984;64(3):351-362.

60. Tosic M, Dimitrijevic R, Mitrovic M. Crystallization of leucite as the main phase in glass doped with fluorine anions. J.Mater.Sci. 2002;37(11):2293-2303.

61. Höland W, Beall G. Glass-ceramic Technology. 2002.

62. Huling JC, Messing GL. Epitactic nucleation of spinel in aluminosilicate gels and its effect on mullite crystallization. J Am Ceram Soc. 1991;74(10):2374-2381.

63. Tkalcec E, Kurajica S, Ivankovic H. Diphasic aluminosilicate gels with two stage mullitization in temperature range of 1200–1300°C. J Eur Ceram Soc. 2005;25(5):613-626.

64. Bischoff C, Eckert H, Apel E, Rheinberger VM, Holand W. Phase evolution in lithium disilicate glass-ceramics based on non-stoichiometric compositions of a multi-component system: structural studies by ^{29}Si single and double resonance solid state NMR. Phys Chem Chem Phys. 2011;13(10):4540-4551.

65. Zhang P, Li X, Yang J, Xu S. The crystallization and microstructure evolution of lithium disilicate-based glass-ceramic. J Non-Cryst Solids. 2014;392:26-30.

66. He P, Jia D, Wang M, Zhou Y. Thermal evolution and crystallization kinetics of potassium-based geopolymer. Ceram Int. 2011;37(1):59-63.

67. Abbot RN. $KAlSiO_4$ stuffed derivatives of tridymite - phase-relationships. Am Mineral. 1984;69(5-6):449-457.

68. Zhang Y, Qu C, Rao P, Lv M, Wu J. Nanocrystalline seeding effect on the crystallization of two leucite precursors. J Am Ceram Soc. 2007;90(8):2390-2398.